from Atmospheric Variations," *Journal of Spacecraft and Rockets*, Vol. 5, No. 8, Aug. 1968. pp. 1005–1007.

[3] Bryson, A. E., Jr. and Ho, Y.-C., "Applied Optimal Control," *AIAA Professional Study Series*, AIAA, New York, Aug. 1967, Chap. 11.

[4] *U.S. Standard Atmosphere*, U.S. Government Printing Office, Dec. 1962.

[5] Allen, H. J. and Eggers, A. J., Jr., "A Study of the Motion and Aerodynamic Heating of Ballistic Missiles Entering the Earth's Atmosphere at High Supersonic Speeds," Rept. 1381, 1958, NACA.

Re-Entry Vehicle Roll Control Utilizing Recirculating Base Flow

M. D. Bennett* and Amado A. Trujillo†
Sandia Laboratories, Albuquerque, N.Mex.

Nomenclature

A = vehicle base area
C_l = rolling moment coefficient, $L/q_\infty Ad$
$C_{N\theta}$ = vehicle normal force coefficient per unit angle of attack, $\partial C_N/\partial\theta$
d = vehicle base diameter
I_x = mass moment of inertia about vehicle longitudinal axis
I_y = mass moment of inertia about vehicle lateral axis
q_∞ = freestream dynamic pressure
S = fin planform area
$x_{c.p.}$ = distance from vehicle's center of mass to center of pressure
y = lateral distance from vehicle's center of mass to axis of aerodynamic symmetry
α_t = nonrolling vehicle trim angle of attack
θ = vehicle resultant angle of attack
$(\dot{\ })$ = denotes differentiation with respect to time

Introduction

Ballistic bodies with small asymmetries about the spin axis may exhibit erratic behavior when the roll and nutational frequencies are approximately equal.[1–4] The roll resonance phenomenon may not pose a serious design problem for a re-entry vehicle of large size because the rotational asymmetries are relatively minor. However, because of the inequality of scaling laws for mass and aerodynamic properties, and the possibility of proportionally more asymmetric ablation of the heatshield or significant thermal distortion of the body, the susceptibility to roll resonance increases as the geometric size of the vehicle decreases or as the ballistic factor increases.[5–8] Control of the vehicle roll position, or its space or time derivatives, is required when it is impractical to restrict the configurational asymmetry enough to prevent persistent roll resonance.

The novel roll-control concept discussed in this Note consists of a number of blades or fins that are attached to the base of the vehicle (Fig. 1) and are oriented such that their reaction to the small, but not insignificant, radial component of the flow along the cone base produces a rolling moment. This control system has several attractive features. The low heat-transfer rates in the region of the fins provide a distinct and important design advantage over systems using conventional, exposed aerodynamic surfaces. Lockman[9] shows that the heat-transfer rate at the center of the base is about two orders of magnitude less than at the nose stagnation point.

Received June 2, 1969; revision received July 31, 1969. This work was supported by U.S. Atomic Energy Commission.

* Staff Member, Aeroballistics Division. Associate Fellow AIAA.

† Staff Member, Experimental Aerodynamics Division. Member AIAA.

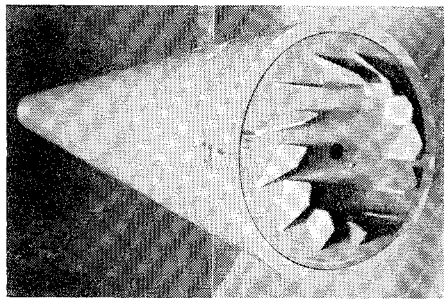

Fig. 1 Re-entry vehicle model in hypersonic wind tunnel showing cone-support strut and base impeller.

Unlike systems that employ control jets, an onboard gas system is not required. The major disadvantage of the system is the limited torque available for the control function.

Wind-Tunnel Tests

Three base impeller configurations were evaluated at zero angle of attack, Mach 7.3, and at a freestream Reynolds number of 0.55×10^6 based on cone base diameter. The model was supported in the test section by a slender, transverse strut to minimize the flow interference effects in the recirculation zone. A portion of the strut can be seen in Fig. 1. The model was a 10° half-angle cone having a 4-in. base diameter and a 0.375-in. nose radius. The boundary-layer flow at the cone base was laminar.

The three impeller configurations are shown in Fig. 2. Configurations A and B each contain 12 fins that have a combined planform area of 2.50 and 3.58-in., respectively; configuration C has 8 fins with a combined area of 5.60-in. The fin span of all three configurations was maintained constant at 0.60-in. or 15% of the cone base diameter.

During tests, the impeller was attached to a shaft mounted on ball bearings located inside the conical model so that the fin assembly could rotate relative to the stationary body. The assembly was locked in position until steady-state flow conditions in the wind tunnel were achieved; then it was remotely released. The rolling moment was calculated from measurements of the angular acceleration of the impeller and the mass moment of inertia of the rotating components. The results were corrected for bearing friction, which amounted to approximately 15% of the maximum aerodynamic driving moment. The bearing friction was determined before each data run by measuring the angular deceleration of the impeller in a vacuum environment.

As may be seen in Figs. 1 and 2, the trailing (outer) edges of the fins are swept forward with respect to the cone axis; the amount of the sweep is 30° measured from a normal to the plane of the cone base. In the initial tests, both the leading and trailing edges were perpendicular to the plane of the cone base, and all three impeller configurations either failed to rotate or rotated opposite to the anticipated direction. Apparently a part of the forebody boundary-layer flow, expanding around the corner of the cone base and entering the recirculation zone, was impinging upon the trailing portion of the

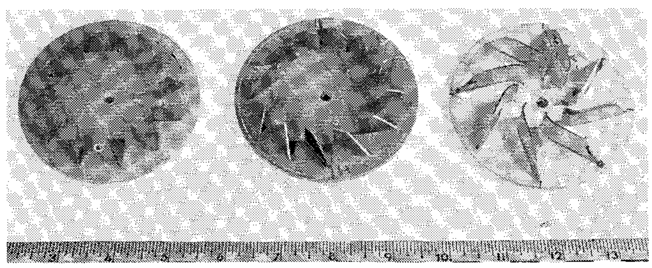

Fig. 2 Experimental base impeller configurations (from left to right, configurations A, B, and C).

Table 1 Experimental rolling moment coefficient

Configuration	Rolling moment coefficient, C_l
A	4.0×10^{-6}
B	6.7×10^{-6}
C	5.3×10^{-6}

fins, thus acting to oppose the driving forces. The situation was corrected by sweeping the fin trailing edges 30°.

During the tests the cone base pressure was measured inside the model to help insure that there were no significant interference effects and that the flow was expanding in a normal manner around the cone-base corner. The ratio of the model base pressure to the tunnel test-section ambient pressure was about 0.20, and comparisons of the measured base-pressure coefficient with other sources of data indicate that the flow in the recirculation zone was not abnormal.[10]

Flight Dynamics

The conditions that produce roll resonance during ballistic flight are functions of the trajectory parameters and of the mass and aerodynamic properties of the vehicle. The criterion for the occurrence of steady roll resonance in circular motion with small angle of attack derived by Vaughn[7] is

$$(2I_y^{1/2}/I_x)(C_{N_\theta}A/x_{\text{c.p.}})^{1/2}(q_\infty^{3/2}/\dot{q}_\infty)(\theta - \alpha_t)y_0 \geq 1 \quad (1)$$

where y_0 is the lateral displacement of the roll axis from the center of mass, and α_t is the out-of-plane aerodynamic trim angle. If Eq. (1) is satisfied, then roll control is necessary, and the magnitude of the required control moment may be estimated by including the rolling moment in the original equation of motion and rederiving the aforementioned criterion. The final result is

$$|C_l| \geq |C_{N_\theta}(\theta - \alpha_t)(y_0/d) - (I_x/I_y^{1/2})(C_{N_\theta}x_{\text{c.p.}}/S)^{1/2}(\dot{q}_\infty/q_\infty^{3/2})(2d^{-1})| \quad (2)$$

where C_l is the dimensionless control moment coefficient. The first term on the right-hand side of the equation is the moment coefficient due to configurational asymmetry, and the other term is due to aerodynamic, inertia, and trajectory effects. The experimental rolling-moment coefficients for the three impeller configurations are shown in Table 1.

Although the maximum possible rolling moment has not been determined in the tests discussed here, an indication of the amount of configurational asymmetry that can be controlled by an optimized impeller design may be obtained by considering the capability of the existing impeller configurations at zero angle of attack. For that purpose it is sufficient to consider only the first term in Eq. (2). By way of example, for a 10° half-angle cone with an 0.1° trim angle in Newtonian flow, the maximum out-of-plane, center-of-mass displacement that can be tolerated for configuration B is $y_0/d = (6.7 \times 10^{-6})(57.3)/(1.96 \times 0.1) = 2.0 \times 10^{-3}$, or 0.048-in. for a 1-ft-radius cone. The inclusion of the remaining term in Eq. (2) will normally increase the permissible configuration asymmetry. However, this increase is not significant for conventional re-entry vehicles unless the trajectory is particularly steep or the dynamic pressure is small. By examining Eq. (2), it may be seen that vehicles with larger configurational asymmetries, and vehicles that are smaller in size, require proportionally larger control moments; further, for $\theta \geq \alpha_t$, an increase in the total angle of attack necessitates a larger control moment.

The characteristics of existing ablation materials and current manufacturing techniques may not be sufficient to maintain the required configurational asymmetry for the assumed vehicle if the ballistic factor is large. Therefore, in practice, either an improved impeller design to provide more control torque or a larger vehicle may be required.

References

[1] Maple, C. G. and Synge, J. L., "Aerodynamic Symmetry of a Projectile," *Quarterly of Applied Mathematics*, Vol. IV, No. 4, Jan. 1949, pp. 345–366.

[2] Nelson, R. L., "The Motions of Rolling Symmetrical Missiles Referred to a Body-Axis System," TN 3737, Nov. 1956, NASA.

[3] Murphy, D. H., "Free Flight Motion of Symmetric Missiles," Rept. 1216, July 1963, Ballistic Research Labs., Aberdeen, Md.

[4] Glover, L. S., "Effects on Roll Rate of Mass and Aerodynamic Asymmetries for Ballistic Re-Entry Bodies," *Journal of Spacecraft and Rockets*, Vol. 2, No. 2, March-April 1965, pp. 220–225.

[5] Pettus, J. J., "Persistent Re-Entry Vehicle Roll Resonance," AIAA Paper 66-49, New York, 1966.

[6] Platus, D. H., "A Note on Re-Entry Vehicle Roll Resonance," *AIAA Journal*, Vol. 5, No. 7, July 1967, pp. 1348–1350.

[7] Vaughn, H. R., "Boundary Conditions for Persistent Roll Resonance on Re-Entry Vehicles," *AIAA Journal*, Vol. 6, No. 6, June 1968, pp. 1030–1035.

[8] Barbera, F. J., "An Analytical Technique for Studying the Anomalous Roll Behavior of Ballistic Re-Entry Vehicles," AIAA Paper 69-103, New York, 1969.

[9] Lockman, W. K., "Free-Flight Base Pressure and Heating Measurements on Sharp and Blunt Cones in a Shock Tunnel," *AIAA Journal*, Vol. 5, No. 10, Oct. 1967, pp. 1898–1900.

[10] Cassanto, J. M., Rasmussen, N. S., and Coats, J. D., "Correlation of Measured Free Flight Base Pressure Data for $M = 4$ to $M = 19$ in Laminar and Turbulent Flow," AIAA Paper 68-699, Los Angeles, Calif., 1968.

Mission Analysis Models for Power-Limited Systems

Robert V. Ragsac*

United Aircraft Research Laboratories, East Hartford, Conn.

IN constructing some mission models for power-limited interplanetary spacecraft systems, the levels of reality employed in characterizing the vehicle system's constituent subsystems and operational constraints are important. This Note discusses some systems analysis models for the purpose of evaluating flight concepts, propulsion mixes and power system performance.

One major guideline was to construct a separate model for each flight mode (not mission); i.e., single-stage operation or mixed-thrust operation, both for a) a given range of powerplant specific mass α_W, b) a given α_W and powerplant mass m_W, and c) given m_W, α_W, and spacecraft gross mass m_0. This approach was employed to gain experience in the synthesis and use of the models and to apply this insight for the development of slightly more general models which allow added refinement and sophistication. The system characterization is a set of equations which describe the net spacecraft mass fraction μ_L, or mass m_L, in terms of the high- and low-thrust propulsion parameters, the trajectory requirements and flight mode. For example, for a single-stage electric propulsion system operating through three gravitational fields,

$$\mu_L = \left[1 + \frac{\alpha_W}{2\eta}\frac{(J_D + J_H + J_C)}{\mu_W}\right]^{-1} - \mu_W \quad (1)$$

Presented at the AIAA 7th Electric Propulsion Conference, Williamsburg, Va., March 3–5, 1969 (no paper number; published in bound volume of meeting papers); submitted April 25, 1969; revision received August 4, 1969.

* Senior Research Engineer.